Iranian Journal of Basic Medical Sciences
ijbms.mums.ac.ir

Electroacupuncture preconditioning alleviates myocardial ischemia-reperfusion injury through reducing the inflammatory response mediated by the miR-146a/TRAF6/IRAK4 pathway

Han Li [1#], Fang-fang Mou [2#], Jing-fan Zhang [3], Meng-ying Huang [1], Jing Zhu [2], Wen Dou [4], Qiang-li Wang [5], Chen-chen Shi [1*], Hai-dong Guo [1, 2*]

[1] Academy of Integrative Medicine, Shanghai University of Traditional Chinese Medicine, Shanghai 201203, China
[2] Department of Anatomy, School of Integrative Medicine, Shanghai University of Traditional Chinese Medicine, Shanghai 201203, China
[3] Department of General Practice, Yuepu Town Community Health Service Center, Shanghai 200941, China
[4] School of Nursing, Shanghai University of Traditional Chinese Medicine, Shanghai 201203, China
[5] Department of Histoembryology, School of Integrative Medicine, Shanghai University of Traditional Chinese Medicine, Shanghai 201203, China

ARTICLE INFO

Article type:
Original

Article history:
Received: Feb 13, 2026
Accepted: Jun 20, 2026

Keywords:
Cardiomyocytes
Electroacupuncture
Inflammatory response
miR-146a
Myocardial ischemic-reperfusion injury

ABSTRACT

Objective(s): Myocardial ischemia-reperfusion injury (MIRI) lacks effective multi-target interventions. Electroacupuncture (EA) shows cardioprotective potential, but its molecular mechanisms remain incompletely understood. This study aimed to investigate whether EA exerts cardioprotective effects by modulating myocardial miR-146a, a microRNA closely associated with inflammation and cardiovascular diseases.

Materials and Methods: A rat model of MIRI was established, and Sprague-Dawley rats were divided into four groups: sham, MIRI, EA treatment, and miR-146a inhibition+EA. Cardiac function, infarct size, myocardial injury, apoptosis, and inflammatory cytokine levels were assessed using echocardiography, TTC staining, CK and LDH assays, TUNEL staining, and ELISA, respectively. The expression and cellular origin of miR-146a were assessed via qRT-PCR, in situ hybridization, and immunofluorescence.

Results: EA treatment significantly improved cardiac function, reduced infarct size, attenuated myocardial injury and apoptosis, and upregulated miR-146a expression in cardiomyocytes. In contrast, inhibition of miR-146a markedly attenuated the protective effects of EA and down-regulated the expression of angiogenic factors bFGF and VEGF, while compromising its anti-inflammatory actions. Furthermore, EA-mediated down-regulation of the inflammatory response was mediated through the miR-146a/TRAF6/IRAK4 pathway.

Conclusion: These findings suggest that EA may alleviate MIRI by upregulating myocardial miR-146a expression, providing novel molecular insights into the cardioprotective mechanisms of EA.

▶Please cite this article as:
Li H, Mou F, Zhang J, Huang M, Zhu J, Dou W, Wang Q, Shi C, Guo H. Electroacupuncture preconditioning alleviates myocardial ischemia-reperfusion injury through reducing the inflammatory response mediated by the miR-146a/TRAF6/IRAK4 pathway. Iran J Basic Med Sci 2026; 29:

Introduction

Myocardial ischemia-reperfusion injury (MIRI) is tissue damage that worsens when blood flow is restored after myocardial ischemia. The main mechanisms include an oxygen free radical burst, calcium overload, inflammatory response, and mitochondrial dysfunction (1). At present, treatment strategies include endogenous protection (such as ischemic preconditioning and post-treatment), drug intervention (such as antioxidants, anti-inflammatory drugs, and mitochondrial protectants), and emerging targeted therapies (such as NAT10 inhibitors and gene therapy). However, most drugs have limited efficacy in clinical trials.

Electroacupuncture (EA) exerts myocardial protection through the integration of neural, immune, and metabolic networks, and has the advantages of a clear mechanism, safe operation, and low cost. It is a potential non-pharmacological intervention in the prevention and treatment of MIRI. EA, especially at the Neiguan acupoint, can exert myocardial protective effects through multiple pathways, including inhibiting the generation of oxygen free radicals, regulating apoptosis-related proteins, reducing inflammatory responses, and activating the vagus nerve cholinergic pathway (inhibiting the inflammatory cascade reaction through α7nAChR)(2-4). In addition, EA pretreatment alleviated MIRI by regulating paraventricular nucleus neurons projecting to the rostral ventrolateral medulla (5). Recent study showed that EA preconditioning conferred protective effects against MIRI in rats by regulating the

*Corresponding authors: Chen-Chen Shi. Academy of Integrative Medicine, Shanghai University of Traditional Chinese Medicine, Shanghai 201203, China. Email: 16111030031@fudan.edu.cn; Hai-Dong Guo. Academy of Integrative Medicine, Shanghai University of Traditional Chinese Medicine, Shanghai 201203, China. Tel/Fax: +86-2151322500. Email: hdguo@shutcm.edu.cn
# These authors contributed equally to this work

mTOR/ROS signaling pathway to inhibit ferroptosis (6). A pilot trial provided evidence for the potential benefits of intraoperative EA in improving microvascular perfusion and preventing or alleviating slow flow/no-reflow during percutaneous coronary intervention in patients with acute myocardial infarction (7). A systematic review and Meta-analysis showed that EA may be a safe and effective strategy to reduce myocardial ischemia-reperfusion injury and speed up the recovery of patients after surgery (8). However, the mechanism of EA in preventing and treating MIRI still needs to be further elucidated.

MiRNA is a type of non-coding RNA that is approximately 22 nucleotides long and participates in the pathogenesis of cardiovascular diseases by regulating gene expression (9). Studies have shown that the abnormal expression of specific miRNAs is closely related to cardiovascular diseases such as myocardial hypertrophy, heart failure, atherosclerosis, and arrhythmia. MiR-146a is a microRNA closely related to inflammation and plays an important role in the occurrence and development of cardiovascular diseases. Research shows that miRNA-146a-5p inhibited hypoxia-induced myocardial fibrosis through endothelial-to-mesenchymal transition (10). In addition, exosomes derived from miR-146a-modified adipose-derived stem cells attenuated myocardial damage via down-regulation of early growth response factor 1 (11). Recently, we found that targeting delivery of miR-146a via IMTP-modified milk exosomes exerted cardioprotective effects by inhibiting the NF-**κB** signaling pathway after MIRI (12). Interestingly, EA treatment may alleviate osteoarthritis by affecting the DNA methylation-regulated transcription of miR-146a and miR-140-5p (13).

In this study, we investigated how EA regulates miR-146a expression in myocardial tissue after MIRI and whether inhibiting miR-146a expression affects EA's role in improving myocardial ischemic injury. In addition, the main source of miR-146a after EA treatment was identified by in situ hybridization. This study will enrich the mechanistic understanding of EA in improving MIRI and provide experimental evidence and theoretical reference for the clinical application of EA in the prevention and treatment of MIRI.

Materials and Methods

Animals

Male Sprague-Dawley (SD) rats weighing 50 g (Used for intramyocardial injection of AAV virus) and 230 g (Used for MIRI model preparation experiments) were purchased from Shanghai Bikai Experimental Animal Co., Ltd. and housed in the Experimental Animal Center of Shanghai University of Traditional Chinese Medicine. The animals were maintained at a specific pathogen-free (SPF) level, with five rats per cage, under a 12:12-hour light-dark cycle (lights on at 7:00, off at 19:00). The room temperature and relative humidity were maintained at 23±1 ˚C and 55±5%, respectively. Food and water were provided *ad libitum*. All animal experimental protocols complied with the regulations on experimental animal management and ethics of Shanghai University of Traditional Chinese Medicine (Approval No. PZSHUTCM2310310005). Moreover, every effort was made to minimize animal suffering and reduce the number of animals used.

MIRI modeling

Following induction of anesthesia with isoflurane (0.4 L/min), SD rats underwent tracheal intubation and thoracotomy to expose the heart. Myocardial ischemia was induced by ligating the left anterior descending coronary artery (LAD) for 30 min, followed by reperfusion upon ligature release. The thoracic cavity was immediately closed (with air evacuation and layered suturing), isoflurane was discontinued, and mechanical ventilation was maintained until spontaneous respiration resumed, after which the endotracheal tube was removed (12, 14). The reperfusion period was set at 4 hr or 24 hr. The procedure of aortic puncture blood sampling and cardiac tissue sampling marks the end of the experiment, which will result in the irreversible death of the animal. Throughout the entire experimental process, all procedures have strictly adhered to the '3R' principles, particularly the principles of reduction and refinement. Experimental animals were maintained under deep anesthesia throughout the process to minimize their suffering.

Electroacupuncture

EA stimulation was applied bilaterally at PC6 (Neiguan, Hand Jueyin Pericardium Meridian) and BL15 (Xinshu, Foot Taiyang Bladder Meridian) using sterile needles (0.25 mm diameter, 0.5 cun length) inserted vertically to a depth of 2.0–3.0 mm. Manual stimulation (lifting, thrusting, and rotating techniques) was performed to elicit deqi, followed by connection to an SDZ-III electroacupuncture device (Suzhou Medical Supplies Factory Co., Ltd.) with a 20 Hz sparse-dense wave at 1 mA intensity. Needles were retained for 30 min under continuous stimulation. For the sham EA treatment, a stainless-steel needle was inserted 2–3 mm into the same points as the pre-EA+MIRI+EA group without electrical stimulation.

Experimental grouping

Five experimental groups were established: Sham group, which underwent sham surgery; MIRI group, subjected to MIRI with 30 min of ischemia followed by 4 hr or 24 hr of reperfusion; Pre-EA+MIRI+EA group, which received 3 days of continuous (EA) intervention before MIRI induction on the fourth day, followed by a single EA treatment; MIRI+EA group, which underwent MIRI followed by a single EA treatment; and AAV+pre-EA+MIRI+EA group, which received AAV viral injection into the myocardium 3 weeks before pre-EA intervention, followed by the same treatments as group.

Preparation of rAAV-CMV-EGFP-WPRE-4XmiR-146a-hGH polyA

The miR-146a gene was amplified using primers with restriction enzyme cutting sites (forward primer 7751-XhoI-F; reverse primer 7751-BglII-R), and the target gene fragment was obtained through PCR amplification. The backbone vector (rAAV-CMV-EGFP-WPRE-hGH polyA) was double-digested with XhoI and BglII to generate a linearized vector fragment. The linearized vector was mixed with the target gene fragment in the correct proportion, and the homologous recombination enzyme Exnase (Basic Seamless Cloning Kit) was added to connect the fragment and the vector through homologous recombination. Finally, transformation screening was carried out, and sequencing verification was performed using the forward sequencing

primer WPRE-178-C-F. After confirming that the inserted fragment was correct and without mutations, the verified positive clones were amplified for plasmid production. The final plasmid rAAV-CMV-EGFP-WPRE-4XmiR-146a-hGH polyA (prokaryotic resistance: Amp) was saved.

Intramyocardial injection

Male SD rats weighing approximately 50 g were anesthetized with isoflurane (0.4 L/min) followed by endotracheal intubation. Adeno-associated virus (AAV, 5.39×10^{12} vg/ml) was injected into the left ventricular wall at a volume of 5 µl per injection site using a 30-gauge needle, with four injection sites administered per rat. After viral injection, intrathoracic air was manually aspirated, and the thoracotomy incision was closed via layered suturing. Mechanical ventilation was maintained while discontinuing isoflurane administration, and ventilator support was continued until spontaneous respiration resumed before tracheal tube removal (15).

Echocardiography

Following anesthesia with isoflurane (0.4 L/min), SD rats were positioned on an ultrasound platform, and a high-frequency transducer was secured to the left chest wall. Using the Vevo2100 imaging system (FUJIFILM Visual Sonics, Canada), M-mode echocardiograms were obtained and recorded. Three consecutive cardiac cycles demonstrating consistent morphology were selected for quantitative analysis of left ventricular function, including measurements of ejection fraction (EF), fractional shortening (FS), left ventricular internal dimensions during diastole and systole (LVIDd, LVIDs), and left ventricular end-diastolic and end-systolic volumes (LVEDV, LVESV) (16).

qRT-PCR

Myocardial tissue for PCR analysis was obtained from the ischemic pale areas in the LAD-supplied region, avoiding non-ischemic areas (such as the right ventricle and posterior wall of the left ventricle) and necrotic core areas. RNA was extracted from tissues from each group using NucleoZOL RNA Extraction Reagent (740404, Company, China). Subsequently, the MiRNA cDNA First-Strand Synthesis Kit (AG11717, Hunan Aikerun Bioengineering Co., Ltd., China) was employed for the reverse transcription reaction. The synthesized cDNA from the reverse transcription was used for subsequent qPCR reactions. The SYBR Green Pro Taq HS Premixed Type qPCR Kit (AG11759, Hunan Aikerun Bioengineering Co., Ltd., China) was utilized for the two-step PCR reaction procedure for detection.

TTC staining

The rat hearts were frozen in a -20 ˚C refrigerator, and after 30 min, they were sliced using a heart matrix (68719, Rayward, China). Each heart was cut into 5 slices, each 1 mm thick. The slices were then immersed in 2% TTC staining solution (G3005, Solarbio, China) and incubated at 37 ˚C for 30 min, and then fixed with paraformaldehyde.

TUNEL

Frozen sections from each group were processed for apoptosis detection using a TUNEL staining kit (C1086, Beyotime, China). After PBS washing, sections were permeabilized with 0.1% Triton X-100 (P0096, Beyotime, China) for 5 min at room temperature, followed by another PBS wash. Sections were then incubated with TUNEL reaction mixture at 37 °C for 1 hour in the dark. Apoptotic cells were visualized and imaged under a fluorescence microscope (Axio Observer 7; ZEISS, Germany).

CK and LDH detection

Under deep anesthesia, whole blood samples were collected via abdominal aorta puncture, followed by immediate cardiac tissue sampling. Serum samples (120 µl) from SD rats in each experimental group were analyzed for creatine kinase (CK) and lactate dehydrogenase (LDH) levels using a fully automated biochemical analyzer (Hitachi 3500, Hitachi High-Tech (Shanghai) Co., Ltd., China).

SOD activity assay

SOD activity in rat serum was measured directly using the assay kit (BC5165, Solarbio Science & Technology, China). The detailed procedure is provided in the reagent instruction manual.

Elisa

Under deep anesthesia, whole blood samples were collected via abdominal aorta puncture. Serum cytokine concentrations (b-FGF, IL-10, VEGF, IL-6, TNF-α, IL-1β) were quantified using commercial ELISA kits (Nanjing Byyan Biological Technology Co., Ltd.; catalog numbers: BY-ER330506, BY-ER330194, BY-ER330908, BY-ER330219, BY-ER331063, BY-ER331206). Following the manufacturer's protocol, standards and test samples were loaded in duplicate wells. After adding 100 µl HRP-conjugated detection antibody, plates were incubated (60 min, 37 ˚C). Five wash cycles (5 min each) with PBS-T were performed before adding 50 µl each of chromogenic substrates A and B (15 min, 37 ˚C). Finally, after adding the stop solution, the readings were measured using a 450 nm enzyme-linked immunosorbent assay instrument (300886376, Tecan Austra GmbA, Australia).

Western blot

Total protein concentration was determined using a BCA protein concentration assay kit (P0009, Beyotime, China). This was followed by electrophoresis (90 V, 45 min) and transfer to film (25 V, 60 min, PVDF membrane). After blocking with 5% skim milk (36120ES76, Yisheng Biotechnology Co., Ltd., China) for 1.5 hr at room temperature, Vinculin antibody (1:1000, S0B1132, STARTER, China), IRAK4 antibody (1:1000, 4363T, CST, USA), IRAK1 antibody (1:1000, 10478-2-AP, Proteintech, China), p-p65 antibody (1:1000, 3033T, CST, USA), p65 antibody (1:1000, 8242T, CST, USA) and TRAF6 antibody (1:1000, 67591T, CST, USA) were incubated overnight at 4 ˚C. The next day, the proteins were incubated with the corresponding horseradish peroxidase (HRP)-labeled secondary antibody (1:3000, 4412; CST, USA) for 1 hr, and the protein bands were developed using an ultrasensitive ECL chemiluminescence kit (P10300, NeoScience, China).

Statistical analysis

The data of this study were statistically analyzed using GraphPad Prism 10 statistical software. The results are presented as mean±standard deviation. Between-group

comparisons were analyzed by one-way ANOVA with Tukey's *post hoc* test. Data normality and homogeneity of variance were confirmed using Shapiro-Wilk and Levene's tests, respectively. When $P<0.05$, the difference between the groups is considered statistically significant.

Results

Pre-EA can improve cardiac function after MIRI

To evaluate the cardioprotective effects of EA in MIRI rats, bilateral PC6 (Neiguan) and BL15 (Xinshu) acupoints were stimulated in four experimental groups: Sham, MIRI, MIRI+EA, and pre-EA+MIRI+EA (Figure 1A). Echocardiographic evaluation at 24-hour reperfusion demonstrated that pre-EA+MIRI+EA treatment significantly enhanced both ejection fraction (EF) and fractional shortening (FS) compared to MIRI and MIRI+EA groups (Figure 1C-D). While MIRI+EA animals showed moderate improvement in cardiac function relative to MIRI controls, the effect was significantly less pronounced than in pre-treated animals. Compared with the MIRI group, there was a downward trend in the LVEDV level of the MIRI+EA group (Figure 1E). Compared with the MIRI group, the level of LVESV in the EA treatment group also decreased, especially in the pre-EA+MIRI+EA group, where the LVESV level showed a significant decrease compared to the MIRI group and the MIRI+EA group (Figure 1F). Similarly, the LVIDd level in the MIRI+EA group was significantly reduced compared to the MIRI group (Figure 1G). The level of LVIDs in the EA treatment group also decreased compared to the MIRI group, especially in the pre-EA+MIRI+EA group, where the LVIDs level showed a significant decrease compared to the MIRI group and the MIRI+EA group (Figure 1H). Sham EA+MIRI rats exhibited no significant difference in EF and FS compared with MIRI rats (Figure S1A-G).

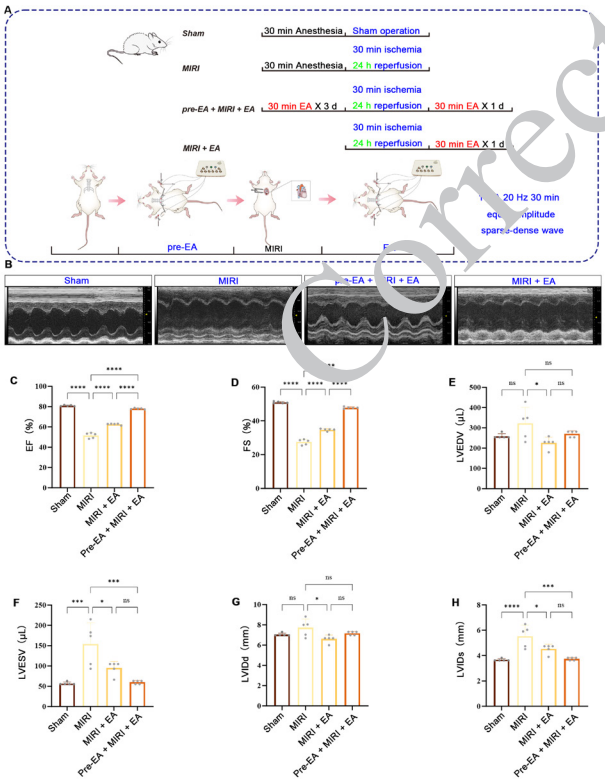

Figure 1. Pre-EA can improve rat cardiac function after MIRI
(A) Experimental grouping schematic. (B-H) Echocardiographic parameters (n=5): cardiac ejection fraction (EF), fractional shortening (FS), left ventricular end-diastolic volume (LVEDV), left ventricular end-systolic volume (LVESV), left ventricular internal diameter at end-diastole (LVIDd), and left ventricular internal diameter at end-systole (LVIDs)
$^{*}P<0.05$, $^{***}P<0.001$, $^{****}P<0.0001$, ns indicates no significance
Pre-EA: Electroacupuncture preconditioning; MIRI: myocardial ischemia-reperfusion injury

Pre-EA can significantly up-regulate the expression of miR-146a in the myocardial injury site

To explore the mechanism of EA in reducing myocardial injury, the expression of miR-146a was detected by qRT-PCR. The data showed that miR-146a expression in myocardial tissue was significantly upregulated in the pre-EA+MIRI+EA group compared to the MIRI group. In contrast, the expression of miR-146a was markedly reduced in the AAV injection group (Figure 2, Figure S2).

Inhibition of miR-146a expression attenuates the improvement of cardiac function by pre-EA

To clarify the regulatory mechanism of miR-146a in EA-mediated myocardial injury repair, an AAV virus targeting miR-146a was constructed. The cardiac function of MIRI rats is significantly decreased after AAV virus intervention (Figure 3A). Compared with the MIRI group, the EF and FS levels in the pre-EA+MIRI+EA group were significantly increased, while the inhibition of miR-146a mediated by the AAV virus could reverse the beneficial effect of pre-EA; the expression levels of EF and FS in the AAV+pre-EA+MIRI+EA group were reduced (Figure 3B-C). Compared with the MIRI group, the expression levels of LVESV, LVEDV, LVIDd, and LVIDs in the pre-EA+MIRI+EA group and the AAV+pre-EA+MIRI+EA group were not significantly changed (Figures 3D-G).

Inhibition of miR-146a attenuates pre-EA reduction of infarct size

TTC staining showed that infarct size was significantly reduced in the pre-EA+MIRI+EA group compared with the MIRI group; however, after myocardial injection of

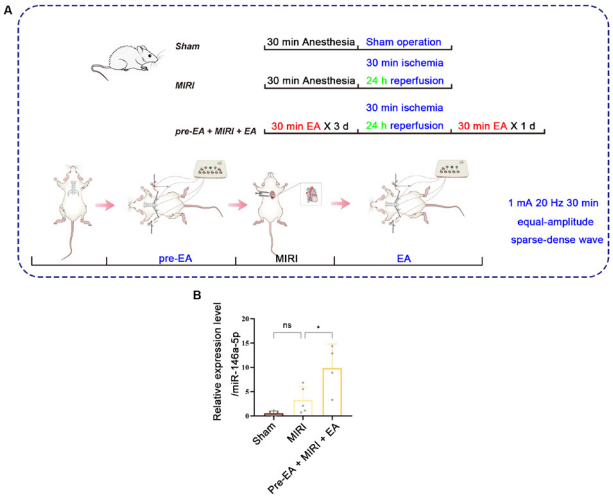

Figure 2. Pre-EA can significantly up-regulate the expression of miR-146a at the site of rat myocardial injury
(A) Experimental schematic diagram. (B) Relative expression of miR-146a measured by quantitative reverse transcription PCR (qRT-PCR)(n=4-5)
$^{*}P<0.05$, ns indicates no significance
Pre-EA: Electroacupuncture preconditioning; miR-146a: microRNA-146a

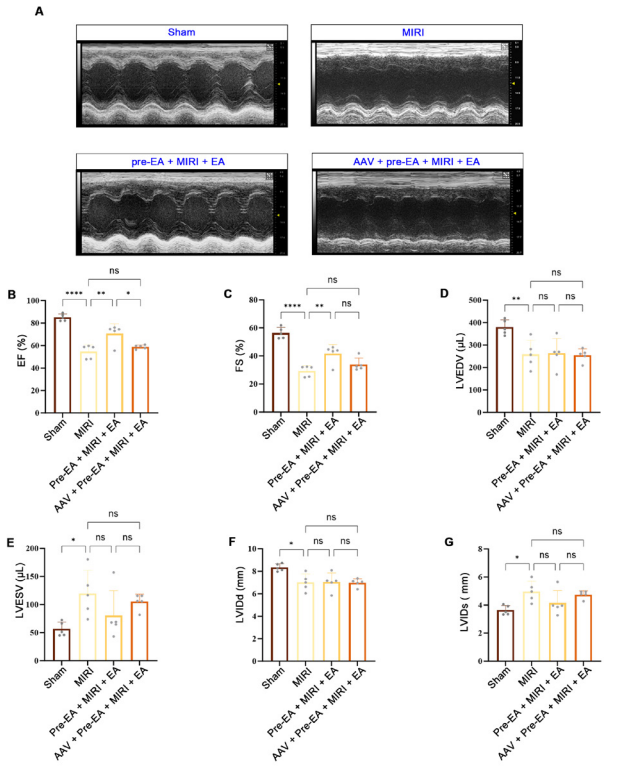

Figure 3. Pre-EA ameliorates rat post-MIRI injury cardiac function via upregulating miR-146a expression
(A-G) Echocardiographic assessment of cardiac function in small animals (n = 5 per group): ejection fraction (EF), fractional shortening (FS), left ventricular end-diastolic volume (LVEDV), left ventricular end-systolic volume (LVESV), left ventricular internal diameter at end-diastole (LVIDd), and left ventricular internal diameter at end-systole (LVIDs)
$^{*}P<0.05$, $^{**}P<0.01$, $^{****}P<0.0001$, ns indicates no significance
Pre-EA: Electroacupuncture preconditioning; MIRI: myocardial ischemia-reperfusion injury; miR-146a: microRNA-146a

AAV virus to specifically inhibit miR-146a expression, EA had a significantly weaker effect on infarct size reduction. The infarct size of the AAV+pre-EA+MIRI+EA group was significantly higher than that of the pre-EA+MIRI+EA group (Figure 4A, B).

Inhibition of miR-146a expression attenuates the regulatory effect of pre-EA on myocardial injury indicators

After 24 hr of perfusion, TUNEL staining showed that myocardial cell apoptosis was significantly reduced in the pre-EA+MIRI+EA treatment group compared with the MIRI group. When the expression of miR-146a was specifically inhibited, the myocardial cell apoptosis rate increased (Figure 5A, B). In addition, we tested myocardial injury indicators in the serum of rats in each group. The experimental data showed that the activities of serum CK and LDH were significantly decreased. At the same time, the levels of antioxidant enzyme SOD were significantly increased in the pre-EA+MIRI+EA group compared with the MIRI group. However, compared with the pre-EA+MIRI+EA group, after inhibiting the expression of miR-146a by injecting AAV virus into the myocardium, the activities of serum CK and LDH were significantly increased, while the levels of antioxidant enzyme SOD were significantly decreased in the AAV+pre-EA+MIRI+EA group (Figure 5C-E). After 4-hour reperfusion, CK, LDH, and SOD levels showed no significant differences among the Sham, MIRI, MIRI+EA, and pre-EA+MIRI+EA groups (Figure S3A-C). TUNEL staining revealed no significant difference in cardiomyocyte apoptosis among the four groups (Figure S3D, E).

Inhibition of miR-146a expression weakens the regulatory effect of pre-EA on cytokine expression

To further investigate whether pre-EA exerted its cardioprotection against MIRI injury via miR-146a, changes in inflammation and pathology of the myocardium were assessed by ELISA and TUNEL. ELISA results showed that compared with the MIRI group, the expression levels of pro-inflammatory factors IL-6, TNF-α, and IL-1β in the serum of the pre-EA+MIRI+EA group are significantly down-regulated. In contrast, the level of anti-inflammatory factor IL-10 is significantly upregulated (Figure 6A-D). Especially, when the expression of miR-146a is specifically inhibited by myocardial injection of AAV virus, the regulatory effect of EA on the expression of inflammatory factors is significantly weakened. In addition, inhibition of miR-146a not only affected the regulation of inflammatory response, but also led to a significant reduction in the expression levels of angiogenesis-related factors bFGF and VEGF. The expression levels of bFGF and VEGF were significantly elevated in the pre-EA+MIRI+EA group compared with the MIRI group (Figure 6E, F). At the same time, this promotion was significantly inhibited by myocardial injection of AAV virus inhibiting the expression of miR-146a. The expression levels of bFGF and VEGF were down-regulated in the AAV+pre-EA+MIRI+EA group.

After 4-hour reperfusion, IL-6 and TNF-α levels

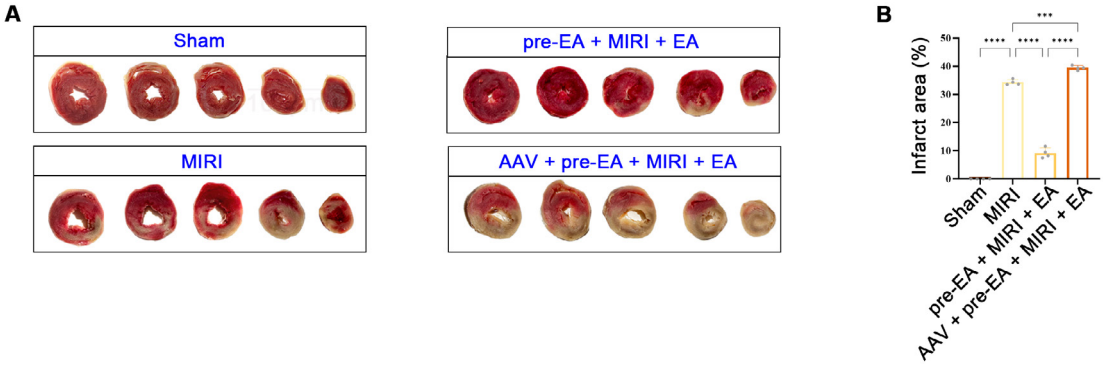

Figure 4. Inhibition of miR-146a attenuates pre-EA reduction of rat infarct size
(A-B) Quantification of myocardial infarct area across experimental groups using triphenyltetrazolium chloride (TTC) staining (n=4)
$^{***}P<0.001$, $^{****}P<0.0001$, ns indicates no significance
Pre-EA: Electroacupuncture preconditioning; MIRI: myocardial ischemia-reperfusion injury; miR-146a: microRNA-146a

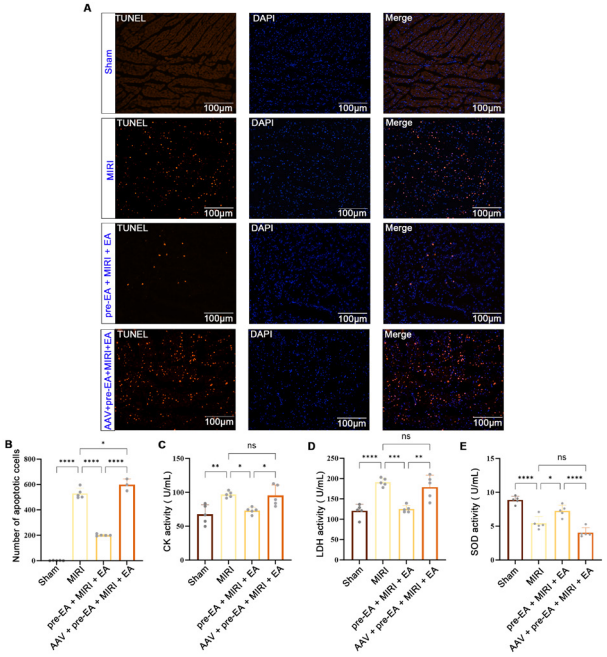

Figure 5. Inhibition of miR-146a expression attenuates the regulatory effect of pre-EA on rat myocardial injury indicators
(A-B) TUNEL assay for apoptosis detection (n=3-5). (C-E) The activities of serum creatine kinase (CK), lactate dehydrogenase (LDH), and superoxide dismutase (SOD) (n=5)
Statistical significance is indicated as $^{*}P<0.05$, $^{**}P<0.01$, $^{***}P<0.001$, $^{****}P<0.0001$; ns indicates no significance
Pre-EA: Electroacupuncture preconditioning; miR-146a: microRNA-146a

showed no significant difference between MIRI and pre-EA+MIRI+EA groups (Figure S4A, B). IL-1β and IL-10 levels were significantly decreased in pre-EA+MIRI+EA compared to MIRI rats (Figure S4C, D). bFGF and VEGF levels showed no significant difference between the two groups (Figure S4E, F).

Electroacupuncture regulates miR-146a/TRAF6/IRAK1 in MIRI

To verify the key mediating role of miR-146a in the anti-inflammatory effect of pre-EA, the TRAF6/IRAK4 /IRAK1 pathway was assessed by western blot. AAV was injected intramyocardially to suppress miR-146a expression, and we examined whether this manipulation attenuated the inhibitory effects of EA on TRAF6, IRAK1, and IRAK4. After 24 hr of reperfusion, western blot analysis revealed that the pre-EA+MIRI+EA group exhibited reduced protein levels of TRAF6, IRAK1, and IRAK4 compared with the MIRI group. However, when miR-146a expression was knocked down by intramyocardial AAV injection, the suppressive effects of EA on TRAF6, IRAK1, and IRAK4 were markedly weakened. Subsequently, we also examined the phosphorylation status of p65, an important downstream marker of NF-κB activation, using Western blot. The p-p65/p65 ratio showed an increasing trend in MIRI rats relative to Sham rats. Pre-EA lowered this ratio, whereas inhibition of miR-146a expression via intramyocardial AAV injection resulted in an elevated p-p65/p65 ratio (Figure 7A-E).

Discussion

Although the cardioprotective effects of EA in MIRI are well documented, its precise molecular mechanisms remain incompletely understood. miR-146a plays a pivotal

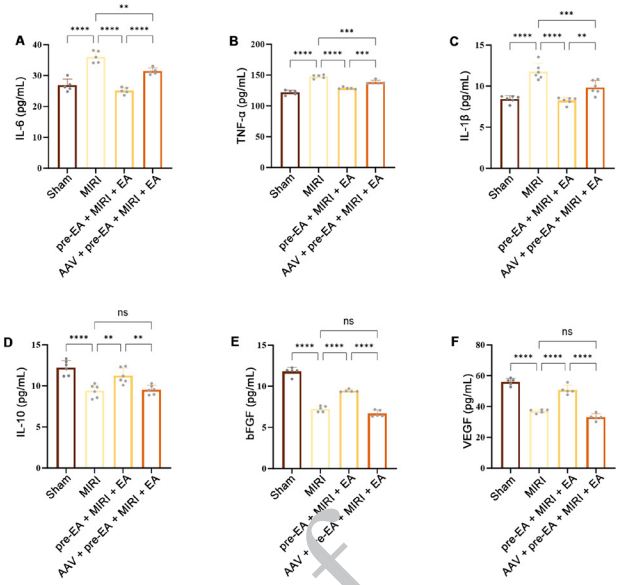

Figure 6. Inhibition of miR-146a expression weakens the regulatory effect of pre-EA on cytokine expression in rats
(A) ELISA kit detection of IL-6 expression (n=5). (B) ELISA kit detection of TNF-α expression (n=5). (C) ELISA kit detection of IL-1β expression (n=6). (D) ELISA kit detection of IL-10 expression (n=5). (E) ELISA kit detection of bFGF expression (n=5). (F) ELISA kit detection of VEGF expression (n = 5)
$^{**}P<0.01$, $^{***}P<0.001$, $^{****}P<0.0001$, ns indicates no significance
Pre-EA: Electroacupuncture preconditioning; miR-146a: microRNA-146a

role in cardiovascular repair by suppressing inflammation, reducing apoptosis, and promoting angiogenesis (17, 18). Our previous study demonstrated that miR-146a delivered via IMTP-modified milk exosomes attenuated MIRI-induced myocardial injury (12). The present study builds on these findings by elucidating that EA upregulates miR-146a to alleviate MIRI through the TRAF6/IRAK4 pathway.

EA exerts multi-target cardioprotection by suppressing inflammation, reducing apoptosis, and modulating

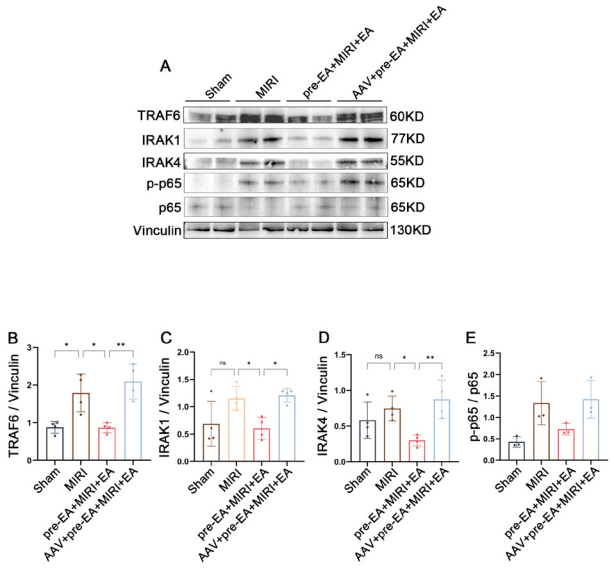

Figure 7. Electroacupuncture reduces TRAF6, IRAK1, IRAK4, and p-p65/p65 expression in rats via miR-146a in MIRI
(A-E) WB detection of TRAF6 and IRAK4 expression at the site of myocardial injury in each group (n=3-4)
$^{*}P<0.05$, $^{**}P<0.01$, ns indicates no significance
Pre-EA: Electroacupuncture preconditioning; MIRI: myocardial ischemia-reperfusion injury; miR-146a: microRNA-146a

oxidative stress (2, 3). PC6 and BL15 are classic acupoints for cardiovascular diseases in TCM theory (19-21). Modern evidence shows that BL15 stimulation improves MIRI by regulating autonomic nervous system function and reducing myocardial enzyme release (22). EA at these points modulates PVN neuronal activity and protects against circulatory dysfunction (21). EA preconditioning at PC6 and BL15 improves post-MIRI cardiac function by enhancing left ventricular efficiency and reducing arrhythmias (23-27). Mechanistically, PC6-EA suppresses sympathetic overactivation and lowers norepinephrine levels (23, 26, 33), while BL15-EA stabilizes autonomic function via hypothalamic PVN modulation (32). Acupuncture point specificity is critical: PC6 and BL15 exhibit specific cardiac protective effects, whereas non-acupoint stimulation does not (3, 21). The selection of PC6 and BL15 is grounded in traditional Chinese medical theory and validated by modern scientific evidence, making them optimal targets for cardiovascular intervention.

miR-146a exerts anti-inflammatory effects by reducing macrophage infiltration and attenuating inflammatory response intensity, as validated in atherosclerosis models (38). In MIRI, miR-146a inhibits the TLR4/NF-κB signaling pathway (39), suggesting its involvement in EA-mediated myocardial protection through dual mechanisms: regulating inflammatory balance and promoting angiogenesis. Our study demonstrated that EA reduced pro-inflammatory factors (IL-6, TNF-α, IL-1β) and promoted angiogenic factors (bFGF, VEGF), exerting cardioprotection through dual anti-inflammatory and pro-angiogenic mechanisms. miR-146a inhibition attenuated both effects, identifying miR-146a as the critical molecular node linking EA stimulation to downstream cardioprotective pathways. Additionally, EA showed significant cardioprotection at 24 hr but limited efficacy at 4 hr post-reperfusion, reflecting the temporal dynamics of MIRI pathological progression: early reperfusion is characterized by acute inflammation and oxidative stress, whereas at 24 hr, tissue enters an active repair phase amenable to EA-mediated modulation of the inflammation-repair balance.

TRAF6 and IRAK4 are core downstream targets of miR-146a-mediated anti-inflammatory effects. TRAF6, as an E3 ubiquitin ligase, cooperates with IRAK4 to activate the NF-κB signaling cascade, driving pro-inflammatory cytokine production (49). miR-146a negatively regulates this pathway by targeting the 3' untranslated regions of TRAF6 and IRAK1/4 (36, 38). Our western blot results demonstrated that EA significantly reduced TRAF6 and IRAK4 protein expression in MIRI myocardial tissue, while miR-146a inhibition reversed this effect, confirming that EA suppresses myocardial inflammation through the miR-146a/TRAF6/IRAK4 axis. This mechanism is consistent with previous studies in liver ischemia-reperfusion injury (50), acute pancreatitis (51), and dry eye disease (52). This study was the first to introduce this classic anti-inflammatory pathway into the mechanism of EA-mediated myocardial protection, providing a novel perspective for understanding the molecular targets of EA.

Although this study established the pivotal role of miR-146a in EA-mediated improvement of MIRI, several limitations should be acknowledged. First, the absence of an AAV-miR-146a inhibition plus MIRI control group without EA limits distinction between the direct effects of miR-146a inhibition and its interaction with EA. Second, the upstream mechanism by which EA upregulates miR-146a remains to be elucidated.

Future research will address these questions and explore whether EA promotes cardiac repair via exosomal miR-146a-mediated stem cell mobilization through the SDF-1/CXCR4 axis (41). In MIRI, inflammation and angiogenesis exhibit dynamic interactions: during ischemia, HMGB1 and IL-1β activate endothelial cells and recruit neutrophils (42, 43); after reperfusion, HIF-1α induces VEGF to promote angiogenesis, whereas ROS impairs vascular function (44), creating a vicious cycle of inflammatory cell infiltration (45). This interaction exhibits time-phase specificity: early TNF-α and IL-6 inhibit angiogenesis (46, 47), while later MCP-1 indirectly promotes angiogenesis by recruiting M2 macrophages (48). Understanding these regulatory mechanisms may provide additional therapeutic targets for MIRI intervention.

Conclusion

This study demonstrates that EA alleviates MIRI by upregulating cardiomyocyte-derived miR-146a expression and modulating the TRAF6/IRAK4 inflammatory pathway. These findings provide molecular evidence for the cardioprotective mechanisms of acupuncture and support miR-146a as a therapeutic target for MIRI intervention.

Acknowledgment

This work was supported by grants from the National Natural Science Foundation of China (No. 82174120) and the Natural Science Foundation of Shanghai (No. 23ZR1460600). The results presented in this paper were part of a student thesis.

Data Availability

The data supporting the findings of this study are available from the corresponding author upon reasonable request.

Ethical Statement

All animal experimental protocols complied with the regulations on experimental animal management and ethics of Shanghai University of Traditional Chinese Medicine (Approval No. PZSHUTCM2310310005).

Authors' Contributions

H L and CC S drafted the paper; MY H, FF M, and J Z corrected the draft and participated in data collection and analysis; H L, JF Z, and W D conducted the experiments; QL W and CC S provided technical assistance and contributed to study design; HD G contributed to supervision of study execution, funding acquisition, and final article approval.

Conflicts of Interest

The authors declare that they have no conflicts of interest.

Declaration

We acknowledge the use of Google Gemini to generate the graphical abstract.

References

1. Wang L, Li D, Yao F, Feng S, Tong C, Rao R, *et al.* Serpina3k lactylation protects from cardiac ischemia reperfusion injury. Nat Commun 2025; 16: 1012.

2. Xia X, Ding Y, Zhou C, Zhang H, Yang X, Shen C, *et al.* Electroacupuncture preconditioning attenuates myocardial ischemia-reperfusion injury in rats partially through Nrf2-mediated reduction of oxidative stress and pyroptosis. Am J Chin Med 2025; 53: 337-352.
3. Zhang J, Yong Y, Li X, Hu Y, Wang J, Wang YQ, *et al.* Vagal modulation of high mobility group box-1 protein mediates electroacupuncture-induced cardioprotection in ischemia-reperfusion injury. Sci Rep 2015; 5: 15503.
4. Zhang H, Liu L, Huang G, Zhou L, Wu W, Zhang T, *et al.* Protective effect of electroacupuncture at the Neiguan point in a rabbit model of myocardial ischemia-reperfusion injury. Can J Cardiol 2009; 25: 359-363.
5. Shu Q, Zhou J, Zhang B, Zhang F, Zhou X, Wu Y, *et al.* Electroacupuncture alleviates myocardial ischemia-reperfusion injury by inhibiting hypothalamic paraventricular nucleus neurons projecting to the rostral ventrolateral medulla. Eur J Neurosci 2024; 60: 4861-4876.
6. Xiao Y, Ding L. Mechanistic study of electroacupuncture preconditioning in alleviating myocardial ischemia-reperfusion injury in rats: Involvement of mTOR/ROS signaling pathway to inhibit ferroptosis. Int J Neurosci 2025; 135: 287-295.
7. Peng Y, Wei X, Wu F, Fan M, Wang K, Zhou J. Electroacupuncture for slow flow/no-reflow phenomenon in patients with acute myocardial infarction undergoing percutaneous coronary intervention: Protocol for a pilot randomized controlled trial. Front Cardiovasc Med 2024; 11: 1401269.
8. Xiaoyu Q, Chunai W, Jianjun X, Jie Z, Xiaoting LU, Shengshuang D, *et al.* Efficacy of electroacupuncture on myocardial protection and postoperative rehabilitation in patients undergoing cardiac surgery with cardiopulmonary bypass: A systematic review and Meta-analysis. J Tradit Chin Med 2024; 44: 1-15.
9. Laggerbauer B, Engelhardt S. MicroRNAs as therapeutic targets in cardiovascular disease. J Clin Invest 2022; 132: e159179.
10. Wang Y, Yu J, Ou C, Zhao Y, Chen L, Cai W, *et al.* miRNA-146a-5p inhibits hypoxia-induced myocardial fibrosis through endMT. Cardiovasc Toxicol 2024; 24: 133-145.
11. Pan J, Alimujiang M, Chen Q, Shi H, Luo X. Exosomes derived from miR-146a-modified adipose-derived stem cells attenuate acute myocardial infarction-induced myocardial damage via downregulation of early growth response factor 1. J Cell Biochem 2019; 120: 4433-4443.
12. Meng WT, Zhu J, Wang YC, Shao CL, Li XY, Lu PP, *et al.* Targeting delivery of miR-146a via RVTP modified milk exosomes exerted cardioprotective effects by inhibiting NF-κB signaling pathway after myocardial ischemia-reperfusion injury. J Nanobiotechnology 2024; 22: 382.
13. Luobin D, Huajun W, Yao LI, Jia LI, Ling LI, Yangping G, *et al.* Electroacupuncture stimulating Neixiyan (EX-LE5) and Dubi (ST35) alleviates osteoarthritis in rats induced by anterior cruciate ligament transaction affecting DNA methylation regulated transcription of miR-146a and miR-140-5p. J Tradit Chin Med 2023; 43: 983-990.
14. Meng WT, Xiao ZX, Li H, Wang YC, Zhao Y, Zhu Y, *et al.* Modified Taohong Siwu decoction improves cardiac function after myocardial ischaemia and reperfusion in rats by promoting endogenous stem cell mobilization and regulating metabolites. Pharm Biol 2022; 60: 1721-1731.
15. Svensson EC, Marshall DJ, Woodard K, Lin H, Jiang F, Chu L, *et al.* Efficient and stable transduction of cardiomyocytes after intramyocardial injection or intracoronary perfusion with recombinant adeno-associated virus vectors. Circulation 1999; 99: 201-205.
16. Li H, Zhu J, Xu YW, Mou FF, Shan XL, Wang QL, *et al.* Notoginsenoside R1-loaded mesoporous silica nanoparticles targeting the site of injury through inflammatory cells improves heart repair after myocardial infarction. Redox Biol 2022; 54: 102384.
17. Xue S, Zhu W, Liu D, Su Z, Zhang L, Chang Q, *et al.* Circulating miR-26a-1, miR-146a and miR-199a-1 are potential candidate biomarkers for acute myocardial infarction. Mol Med 2019; 25: 18.
18. Zhai K, Deng L, Wu Y, Li H, Zhou J, Shi Y, *et al.* Extracellular vesicle-derived miR-146a as a novel crosstalk mechanism for high-fat induced atherosclerosis by targeting SMAD4. J Adv Res 2025; 73: 729-741.
19. Zeng J, Cao J, Yang H, Wang X, Liu T, Chen Z, *et al.* Overview of mechanism of electroacupuncture pretreatment for prevention and treatment of cardiovascular and cerebrovascular diseases. CNS Neurosci Ther 2024; 30: e14920.
20. Wei W, Qingling LI, Qiang MA, Ran X, Bing G, Yi W, *et al.* Effects of moxibustion at bilateral Feishu (BL13) and Xinshu (BL15) combined with benazepril on myocardial cells apoptosis index and apoptosis-related proteins cytochrome c and apoptosis-inducing factor in rats with chronic heart failure. J Tradit Chin Med 2022; 42: 227-233.
21. Wang J, Zhang Q, Yao L, He T, Chen X, Su Y, *et al.* Modulating activity of PVN neurons prevents atrial fibrillation induced circulation dysfunction by electroacupuncture at BL15. Chin Med 2023; 18: 135.
22. Achilli F, Malafronte C, Cesana F, Maggiolini S, Mauro C, De Ferrari GM, *et al.* Granulocyte colony stimulating factor for large anterior ST-elevation myocardial infarction: rationale and design of the prospective randomized phase III STEM-AMI OUTCOME trial. Am Heart J 2015; 170: 652-658.
23. Xi H, Li X, Zhang Z, Cui X, Zhu B, Jing X, *et al.* Continuous peripheral electrical nerve stimulation improves cardiac function via autonomic nerve regulation in MI rats. Heart Rhythm 2024; 21: 2010-2019.
24. Karwi QG, Bice JS, Baxter GF. Pre- and postconditioning the heart with hydrogen sulfide (H(2)S) against ischemia/reperfusion injury *in vivo*: A systematic review and meta-analysis. Basic Res Cardiol 2018; 113: 6.
25. Silva M, Lustosa TC, Arai VJ, Couto Patriota TLG, Lira MPF, Sins-Filho OL, *et al.* Effects of acupuncture on obstructive sleep apnea severity, blood pressure control and quality of life in patients with hypertension: A randomized controlled trial. J Sleep Res 2020; 29: e12954.
26. Ye Z, Zhu L, Li XJ, Gao HY, Wang J, Wu SB, *et al.* PC6 electroacupuncture reduces stress-induced autonomic and neuroendocrine responses in rats. Heliyon 2023; 9: e15291.
27. Luo Z, Wu F, Xue E, Huang L, Yan P, Pan X, *et al.* Hypoxia preconditioning promotes bone marrow mesenchymal stem cells survival by inducing HIF-1α in injured neuronal cells derived exosomes culture system. Cell Death Dis 2019; 10: 134.
28. Blackwood EA, Azizi K, Thuerauf DJ, Paxman RJ, Plate L, Kelly JW, *et al.* Pharmacologic ATF6 activation confers global protection in widespread disease models by reprograming cellular proteostasis. Nat Commun 2019; 10: 187.
29. Martin JL, Costa ASH, Gruszczyk AV, Beach TE, Allen FM, Prag HA, *et al.* Succinate accumulation drives ischaemia-reperfusion injury during organ transplantation. Nat Metab 2019; 1: 966-974.
30. Zhou J, Zhang B, Zhou X, Zhang F, Shu Q, Wu Y, *et al.* Electroacupuncture pretreatment mediates sympathetic nerves to alleviate myocardial ischemia-reperfusion injury via CRH neurons in the paraventricular nucleus of the hypothalamus. Chin Med 2024; 19: 43.
31. Acar HV. Acupuncture and related techniques during perioperative period: A literature review. Complement Ther Med 2016; 29: 48-55.
32. Li F, He T, Xu Q, Lin LT, Li H, Liu Y, *et al.* What is the acupoint? A preliminary review of Acupoints. Pain Med 2015; 16: 1905-1915.
33. Zhou W, Ko Y, Benharash P, Yamakawa K, Patel S, Ajijola OA, *et al.* Cardioprotection of electroacupuncture against myocardial ischemia-reperfusion injury by modulation of cardiac norepinephrine release. Am J Physiol Heart Circ Physiol 2012; 302: H1818-1825.
34. Ji C, Song F, Huang G, Wang S, Liu H, Liu S, *et al.* The protective effects of acupoint gel embedding on rats with myocardial ischemia-reperfusion injury. Life Sci 2018; 211: 51-62.
35. Wang X, Chen Y, Zhao Z, Meng Q, Yu Y, Sun J, *et al.* Engineered

exosomes with ischemic myocardium-targeting peptide for targeted therapy in myocardial infarction. J Am Heart Assoc 2018; 7: e008737.
36. Taganov KD, Boldin MP, Chang KJ, Baltimore D. NF-kappaB-dependent induction of microRNA miR-146, an inhibitor targeted to signaling proteins of innate immune responses. Proc Natl Acad Sci U S A 2006; 103: 12481-12486.
37. Zhang T, Ma Y, Gao L, Mao C, Zeng H, Wang X, *et al.* MicroRNA-146a protects against myocardial ischaemia reperfusion injury by targeting Med1. Cell Mol Biol Lett 2019; 24: 62.
38. Ardinal AP, Wiyono AV, Estiko RI. Unveiling the therapeutic potential of miR-146a: Targeting innate inflammation in atherosclerosis. J Cell Mol Med 2024; 28: e70121.
39. Phu TA, Ng M, Vu NK, Gao AS, Raffai RL. ApoE expression in macrophages communicates immunometabolic signaling that controls hyperlipidemia-driven hematopoiesis & inflammation via extracellular vesicles. J Extracell Vesicles 2023; 12: e12345.
40. Pan JA, Tang Y, Yu JY, Zhang H, Zhang JF, Wang CQ, *et al.* miR-146a attenuates apoptosis and modulates autophagy by targeting TAF9b/P53 pathway in doxorubicin-induced cardiotoxicity. Cell Death Dis 2019; 10: 668.
41. Liesveld JL, Sharma N, Aljitawi OS. Stem cell homing: From physiology to therapeutics. Stem Cells 2020; 38: 1241-1253.
42. Andrassy M, Volz HC, Igwe JC, Funke B, Eichberger SN, Kaya Z, *et al.* High-mobility group box-1 in ischemia-reperfusion injury of the heart. Circulation 2008; 117: 3216-3226.
43. Timmers L, Pasterkamp G, de Hoog VC, Arslan F, Appelman Y, de Kleijn DP. The innate immune response in reperfused myocardium. Cardiovasc Res 2012; 94: 276-283.
44. Guo J, Wang S, Wan X, Liu X, Wang Z, Liang C, *et al.* Mitochondria-derived methylmalonic acid aggravates ischemia-reperfusion injury by activating reactive oxygen species-dependent ferroptosis. Cell Commun Signal 2024; 22: 53.
45. Semenza GL. Oxygen sensing, hypoxia-inducible factors, and disease pathophysiology. Annu Rev Pathol 2014; 9: 47-71.
46. Frangogiannis NG. The inflammatory response in myocardial injury, repair, and remodelling. Nat Rev Cardiol 2014; 11: 255-265.
47. Van der Heiden K, Cuhlmann S, Luong le A, Zakkar M, Evans PC. Role of nuclear factor kappaB in cardiovascular health and disease. Clin Sci (Lond) 2010; 118: 593-605.
48. Wynn TA, Vannella KM. Macrophages in tissue repair, regeneration, and fibrosis. Immunity 2016; 44: 450-462.
49. Cohen P, Strickson S. The IRAK-catalysed activation of the E3 ligase function of TRAF6. Biochem J 2017; 474: 1577-1593.
50. Bian Z, Li L, Cui J, Lu Y, Ding W, Liu G, *et al.* miR-146a ameliorates liver ischemia/reperfusion injury by suppressing IRAK1 and TRAF6. PLoS One 2014; 9: e101530.
51. Zhang L, Li Y, Wang Y, Xia L, Wan J. MiR-146a reduces inflammation in experimental pancreatitis via the TRAF6–NF-κB signaling pathway. Immun Inflamm Dis 2025; 13: e70163.
52. Han R, Li Y, Wang Y, Hao P, Chen X, Wang Y, *et al.* MicroRNA-146a negatively regulates inflammation via the IRAK1/TRAF6/NF-κB signaling pathway in dry eye. Sci Rep 2023; 13: 11346.